Synthesis, Dielectric, and Photochemical Study of Liquid Crystalline Main Chain Poly(ester imide)s Containing Cinnamoyl Moieties

Beate Sapich and Joachim Stumpe*

Institute of Thin Film Technology and Microsensorics, Erieseering 42, D-10319 Berlin, Germany

Hans R. Kricheldorf

Institute of Technical and Macromolecular Chemistry, University Hamburg, Bundesstrasse 45, D-20146 Hamburg, Germany

Andreas Fritz and Andreas Schönhals

Federal Institute of Material Research and Testing, Unter den Eichen 87, D-12205 Berlin, Germany

Received September 19, 2000; Revised Manuscript Received April 16, 2001

ABSTRACT: Photochromic liquid crystalline main chain poly(ester imide)s with cinnamoyl moieties and chiral groups as part of the backbone were characterized concerning their liquid crystalline, molecular dynamical, and photochemical properties. Homo- and copolymers were synthesized by polycondensation of mixtures containing isosorbide, *tert*-butylhydroquinone, or catechol. The copolyesters were cholesteric, but exclusively the polymers containing the *tert*-butylhydroquinone moiety form Grandjean textures on annealing. These polymer films show blue iridescent color. UV irradiation causes photo-cross-linking of the polymers via the (2 + 2) photocycloaddition of the cinnamoyl moieties, resulting in insoluble films in which the iridescent supramolecular structure is frozen in without any changes compared to the initial films. Dichroism of about 0.07 is induced upon irradiation with linearly polarized UV light. In contact with liquid crystals, the photoinduced anisotropic interface of the films causes an efficient alignment of liquid crystals.

Introduction

Cholesteric polymers have interesting optical properties which are useful for optically active films, coatings, or pigments. The application of cholesteric polymers for such purpose requires the combination of two properties in these materials. First, the LC polymers should form aligned films of good quality. The second requirement is the stabilization of the supramolecular structure by high glass transition temperatures or the stabilization of reactive cholesteric monomers by photopolymerization or, alternatively, the photo-cross-linking of cholesteric polymers containing photo-cross-linkable moieties. Under this aspect the photo-cross-linking of cholesteric polyester and poly(ester imide)s containing cinnamoyl groups forming iridescent Grandjean texture[1,2] has been studied.

Rubbed polyimide films are well-known as the aligning layer in the LC display production. However, the conventional rubbing technique has many disadvantages, such as the formation of electrostatic charges and of dust particles. The photoinduced alignment of LC molecules has recently received much attention, overcoming these disadvantages.[3] Moreover, the photoalignment technique allows the patterned orientation of subpixels with different orientational directions in contrast to all other techniques. In that way, new types of displays can be developed. Several materials and methods have been proposed for the photoalignment technology. The photoinduced anisotropy can be generated by angular-selective photodimerization of −CH═CH− double bonds such as for poly(vinyl cinnamate)[4−7] or by other angular-selective decomposition reactions as in the case of polyimides.[7−10] The photoorientation in the steady state of a photoisomerization process is an alternative mechanism by which the photochromic moieties change their orientation, but they are rebuilt on the molecular level while the induced direction remains stable. Polyimides and poly(viny cinnamte)s are the two classes of polymers, which are most promising for the photoalignment technique. The studied cinnamoyl-containing poly(ester imide)s combine structure elements of both classes, so it will be interesting to check their photoalignment capability.

In general, rigid main chain polymers can have a quite complex morphology. So for instance, PET/*x*PHB copolyesters (PET = poly(ethylene terephthalate), PHB = *p*-hydroxybenzoic acid) have for $x > 0.25$ a hierarchical micromorphology consisting in crystalline, liquid crystalline, and amorphous microdomains (see for instance ref 11 and references quoted there). In the case of poly(ethylene 2,6-naphthalene dicarboxylate) (PEN) which is quite similar to PET but having a naphthalene instead of a phenyl group, it was found by optical spectroscopy that the naphthalene moieties are aggregated in *solution* as well as in the *dense* state,[12,13] which led to more complex relaxation behavior compared to the case of PET.[14,15] Also for novel poly(amide imide)s WAXS investigations indicate a paracrystalline order.[16]

Dielectric spectroscopy is a powerful method to characterize the molecular dynamic behavior of polymeric systems.[17] Obviously, a definite molecular mobility is necessary for the most photoreactions in the dense state of polymers. This is more important for bimolecular reactions[18] and for the induction of anisotropy by photoorientation.[19−21] But it should be noted that the interplay of molecular photoreactions, generation of

* To whom the correspondence should be addressed.

10.1021/ma001616b CCC: $20.00
Published on Web 07/03/2001

Table 1. Yields and Properties of the Model Esters 1−4

form	yield [%]	elem form [form wt]		elemental analyses C	H	N	mp [°C]
1	52.8	$C_{16}H_{18}O_4$	calcd	70.07	6.57		86
		[274]	found	70.48	6.43		
2	42.6	$C_{26}H_{22}O_6$	calcd	72.56	5.12		212
		[430]	found	73.50	5.01		
3	30.3	$C_{22}H_{19}NO_6$	calcd	67.17	4.83	3.56	160
		[395]	found	66.94	4.85	3.56	
4	39.7	$C_{32}H_{23}NO_8$	calcd	69.94	4.19	2.55	242
		[549]	found	69.28	4.23	3.00	

anisotropy, and molecular mobility is still poorly understood and remains an actual topic of basic research. Therefore, optical spectroscopy is combined with dielectric relaxation spectroscopy in this paper.

The aim of this study is the stabilization of a chiral supramolecular structure and the photoinduction of anisotropy in polymer films with respect to the dynamics and the photochemical properties of this new class of poly(ester imide)s.

Experimental Section

Materials. Methylhydroquinone, 4-hydroxybenzaldehyde, 4-hydroxyacetophenone, and isosorbide were purchased from Aldrich Co. (Milwaukee, WI) and used without further purification. Isosorbide was dried over P_4O_{10} in a vacuum prior to use. All solvents were purified and dried by the usual methods before use.

Synthesis of Monomers and Model Compounds. The synthesis of *N*-(4-carboxyphenyl) trimellitimide, *N*-(4-chlorocarbonylphenyl) trimellitimide chloride, *N*-(4-[2-carboxyethenyl]phenyl) trimellitimide, *N*-(4-[2-chlorocarbonylethenyl]-phenyl) trimellitimide chloride, and *p*-phenylenebis(acrylic acid) dichloride were prepared according to the literature.[22−25]

Diethyl-p-phenylene Bis(acrylate), **1** (see Table 1). *p*-Phenylene bis(acrylic acid) dichloride (0.06 mol) was dissolved in an excess of dry ethanol (10 mL). The solution was heated 24 h until the end of the HCl evolution. After cooling the crystals were isolated by filtration and washed with ligroin.

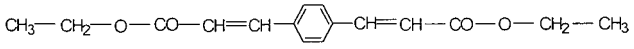

1

Bis(4-methoxyphenyl-p-phenylene) Bis(acrylate), **2** (see Table 1). *p*-Phenylene bis(acrylic acid) dichloride (0.06 mol), hydroxyanisole (0.13 mol), and pyridine (9 mL) were heated in dry DMF at 120 °C for 20 h with stirring. After cooling the solution was poured into ice water. The crystallized product was isolated and washed with water.

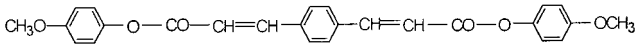

2

Diethyl Ester of 4-Aminocinnamic Acid Trimellitimide, **3** (see Table 1). *N*-(4-[2-Chlorocarbonylethenyl]phenyl) trimellitimide dichloride (0.013 mol) and dry ethanol (10 mL) were refluxed for 20 h. After cooling the crystallized product was isolated by filtration and washed with ligroin.

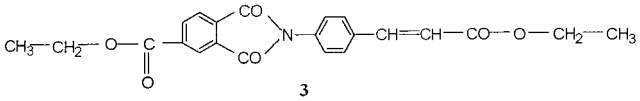

3

Bis(4-methoxyphenyl) Ester of 4-Aminocinnamic Acid Trimellitimide, **4** (see Table 1). *N*-(4-[2-Chlorocarbonylethenyl]-phenyl) trimellitimide dichloride (50 mmol), hydroxyanisole (130 mmol), and pyridine (9 mL) are stirred in dry DMF (15 mL) at 120 °C for 20 h. After cooling the solution was poured into ice water. The precipitated product was isolated and washed with water.

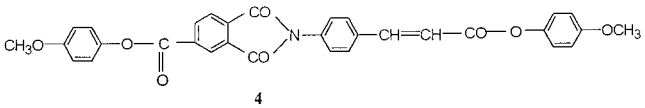

4

Polycondensation Reactions. The dichloride of 4-aminocinnamic acid trimellitimide (8 mmol), adipoyl chloride (2 mmol), catechol, or *tert*-butylhydroquinone (9.5 mmol) and isosorbide (0.5 mmol) were weighed into a cylindrical glass reactor equipped with a glass inlet and outlet tubes. Dry 1-chloronaphthalene (15 mL) was added. The reactor was placed into an oil bath preheated to 210 °C, and the reaction mixture was homogenized with a mechanical stirrer. The reaction time was 24 h. Finally, the product was dissolved in 50 mL of a mixture of CH_2Cl_2 and trifluoroacetic acid (4/1 by volume), precipitated into methanol, and dried at 60 °C in a vacuum. All other polycondensation reactions were carried out in the same manner.

Sample Preparation. The monomers were dissolved in $CHCl_3$, and the polymers were solved in a mixture of chloroform and trifluoroacetic acid (4/1 by volume). Films were prepared by casting these solutions on glass substrates. The preparation of the films was difficult due to restricted solubility of the polymers and adhesion effects.

Measurements. The inherent viscosities were measured with an automated Ubbelohde viscosimeter thermostated at 20 °C. In each case a solution of 100 mg of the related poly(ester imide) in the mixture CH_2Cl_2/TFA (4/1 by volume, 50 mL) was used for the measurements.

The DSC measurements were carried out using a Perkin-Elmer DSC-4. All measurements were done with a heating and a cooling rate of 20 K/min under nitrogen.

The ^{1}H NMR spectra were recorded using a Bruker AC-100 FT NMR spectrometer. The samples were given in 5 mm o.d. sample tubes. A 4/1 mixture (by volume) of $CDCl_3$/TFA containing TMS served as solvent and shift reference.

The optical rotation was measured with a Perkin-Elmer 241 polarimeter in a cuvette with 100 mm length using a polyimide concentration of 2 g/L in CH_2Cl_2/TFA as solvent mixture (4/1 by volume) at 20 °C.

The UV irradiation (313 nm, 2,7 mW/cm^2) was carried out using a 100 W HBO lamp, metal interference filter, and a cuvette filled with water to remove the IR irradiation. The change of UV/vis absorption was measured using a UV/vis spectrometer LAMBDA 2 (Perkin-Elmer).

The polarized irradiation was carried out using a HeCd laser with a wavelength of 325 nm and a power of 10 mW/cm^2.

For the dielectric spectroscopy the samples were pressed at a temperature of about 500 K between two gold-plated stainless steel electrodes with a spacing of 50 μm maintained by fused silica fibers. The equipment to measure the dielectric function $\epsilon^*(f) = \epsilon'(f) - i\epsilon''(f)$ (f = frequency, ϵ' = real part, ϵ'' = imaginary or loss part, $i = \sqrt{-1}$) in a frequency range from 10^{-1} to 10^5 Hz is described elsewhere.[26] The temperature is varied from 173 to 493 K. All measurements are carried out under isothermal conditions.

Results and Discussion

Synthesis. All polymers were prepared by the same procedure. The dichloride of *p*-phenylene diacrylic acid was heated with a mixture of isosorbide and a selected diphenol in 1-chloronaphthalene (**5a,c** and **6a,c**). The liberated hydrogen chloride was removed with a slow stream of nitrogen.

The copolymers **7a**−**c** and **8a**−**c** were prepared by the polycondensation of *N*-(4-[2-chlorocarbonylethenyl]phenyl) trimellitimide chloride with a diphenol and isosorbide. The yields and relevant properties of the copoly(ester imide)s are summarized in Table 2.

Table 2. Yields and Properties of the Copolyimides

form	yield [%]	elem form [form wt]		elemental analyses C	H	N	η_{inh}[a] [dL/g]	$[\alpha]_D^{20}$ [deg]
5a	83.7	$C_{238}H_{192}N_5O_{51}$	calcd	72.60	4.88	1.78	0.33	−34.5
		[3934]	found	71.14	4.91	1.68		
5c	60.0	$C_{218}H_{125}O_{41}$	calcd	75.41	5.68		0.31	−33.0
		[3397]	found	74.40	5.87			
6a	85.6	$C_{200}H_{116}N_5O_{51}$	calcd	70.55	3.41	2.06	0.20	−24.9
		[3402]	found	69.82	3.50	1.98		
6c	65.8	$C_{180}H_{121}O_{41}$	calcd	73.54	4.11		0.21	−32.2
		[2937]	found	72.39	4.20			
7a	57.0	$C_{230}H_{203}N_6O_{53}$	calcd	70.86	5.21	2.16	0.41	−22.8
		[3895]	found	69.99	5.18	2.09		
7b	86.0	$C_{254}H_{205}N_8O_{57}$	calcd	70.26	4.79	2.62	1.12	−13.9
		[4277]	found	69.61	4.68	2.57		
7c	89.3	$C_{278}H_{207}N_{10}O_{61}$	calcd	71.60	4.44	3.00	1.08	−19.6
		[4659]	found	71.03	4.38	2.94		
8a	66.6	$C_{192}H_{127}N_6O_{53}$	calcd	68.51	3.78	3.50	0.30	−27.3
		[3363]	found	68.62	3.47	3.38		
8b	57.9	$C_{216}H_{129}N_8O_{57}$	calcd	69.21	3.44	2.99	0.29	−21.8
		[3745]	found	68.70	3.56	2.78		
8c	75.0	$C_{240}H_{131}N_{10}O_{61}$	calcd	68.78	3.89	2.39	0.32	−23.0
		[4127]	found	67.89	4.01	2.40		

[a] Measured at 20 °C, with $c = 2$ g/L in CH_2Cl_2/TFA (volume ratio 4/1).

All copolyesters of this work were prepared with 5% of isosorbide, because all previous studies of isosorbide-containing copolyesters have shown that higher fractions are unfavorable for the formation of a Grandjean texture.[24,27−29] Isosorbide is known[29] to possess a high helix twisting power, and obviously, a high molar fraction of isosorbide generates helices with a pitch which is too small for the interaction with visible light. The substituted hydroquinones were selected as diphenols because the para position of the hydroxy groups favors the formation of LC phases and because substituted hydroquinones have proven in previous studies[30] to favor the formation of noncrystalline cholesteric poly(ester imide)s. In contrast, the incorporation of catechol results in amorphous copoly(ester imide)s as expected from similar studies of catechol countaining LC polyesters.[31] The chemical structure and composition of all polyesters were checked by elemental analyses (see Table 2) and by IR and ^{1}H NMR spectroscopies. The elemental analyses showed the greatest difference of calculated and experimental values for the C atoms. However, the difference never exceeded 1%. The IR spectra exhibited the band of CH═CH stretch vibrations at 1640 cm^{-1}, the C═O stretching vibration of the ester groups around 1715 cm^{-1}, and an additional, but weak, C═O band of the imides rings at 1740 cm^{-1}. The 400 MHz ^{1}H NMR spectra proved in all cases a composition according to the feed ratios. Figure 1 presents a NMR spectrum with signal assignments as a typical example.

Properties. All synthesized copoly(ester imide)s **5**−**8** are liquid crystalline. The thermal properties were determined by polarizing optical microscopy and DSC measurements. The data of the glass transition temperatures, T_g, the clearing temperatures, T_{cl}, at which the isotropization of the film takes place, and the degradation temperatures, T_d, at which the polymers becomes thermally destroyed are summarized in Table 3.

Polymers **5** and **6** containing the *p*-phenylene diarylic moiety show a decreases of T_g for the copolymers with regard to the homopolymers. In the cases of polymers **7** and **8** the effect is reverse. The incorporation of 20% and 40% adipinic acid in the copolymer results in a significant decrease of the glass transition temperature compared to the case of homopolymer **8c**.

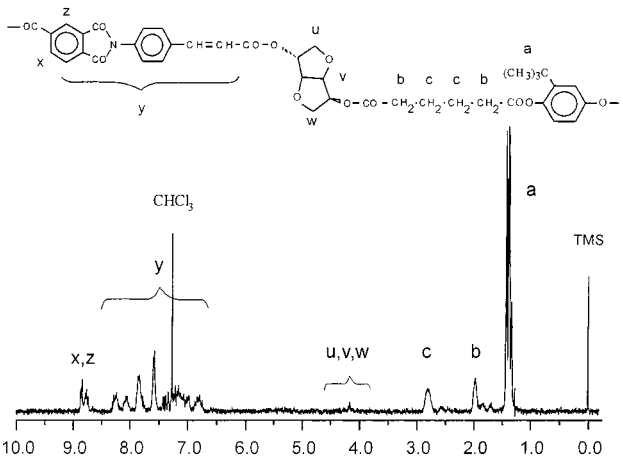

Figure 1. ^{1}H NMR spectra of **7a**.

Table 3. Thermal Properties of the Polymers

polymer	T_g [°C]	T_{cl} [°C]	T_d [°C]	texture
5a	168	180	>400	Grandjean (blue)
5c	159	200	>400	nematic Schlieren
6a	168	190	>380	nematic Schlieren
6c	167	200	280−330	nematic Schlieren
7a	175	180	>400	Grandjean (blue)
7b	179	215	350−380	Grandjean (blue)
7c	200	220	>400	cholesteric
8a	129	160	270−290	LC
8b	134	160	260−290	LC
8c	184	180	280−290	LC

All polymers **5**−**8** are liquid crystalline. Polymers **5c**, **6a**, and **6c** form nematic mesophases visualized by Schlieren textures, while **5a** and **7a**−**c** are cholesteric. But Grandjean textures were only found in the case of copoly(ester imide)s **5a, 7a,** and **7b** containing *tert*-butylhydroquinone. The copolymers were prepared with small quantities of isosorbide, because formulations with molar fractions above 15% (relative to the sum of the diols) do not form Grandjean textures.[24,27−30] The LC phases of **8a** and **8c** are not characterized so far.

Dielectric Spectroscopy. Dielectric spectroscopy provides information about molecular motions related to fluctuation of dipoles. For amorphous polymers below T_g in the glassy state a so-called β-relaxation process

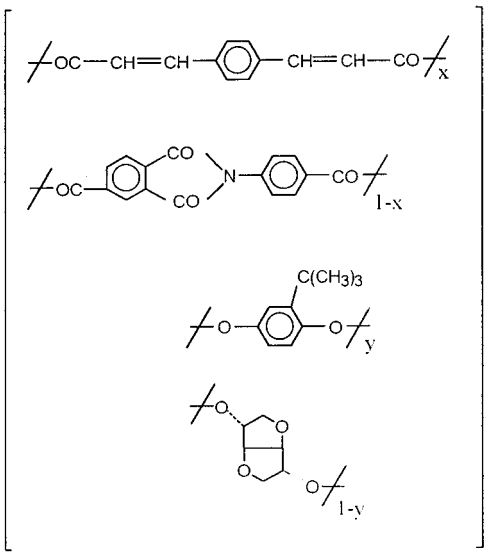

5

5a: x=0.5
y=0.95
5c: x=1
y=0.95

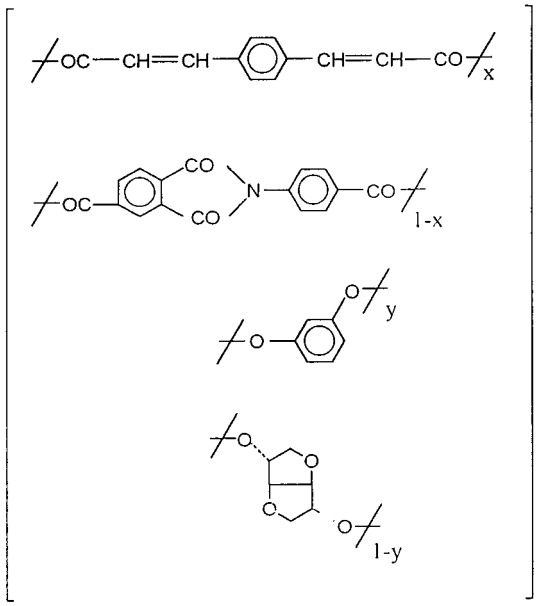

6

6a: x=0.5
y=0.95
6c: x=1
y=0.95

takes place, which is related to local rotational fluctuations of polar groups.[17] The temperature dependence of the relaxation rates or times of the β process follows an Arrhenius equation. Above T_g the α-relaxation or dynamic glass transition mainly connected with the segmental motions[17] can be observed. The temperature dependence of its relaxation rates is in general non-Arrhenius and corresponds to the glass transition temperature at low frequencies. For rigid main chain polymers (or copolymers) the behavior can be more complex. So for instance two dynamic glass transitions could be observed for PET/*x*PHB copolyesters which indicate a microphase-separated structure.[11] In addition

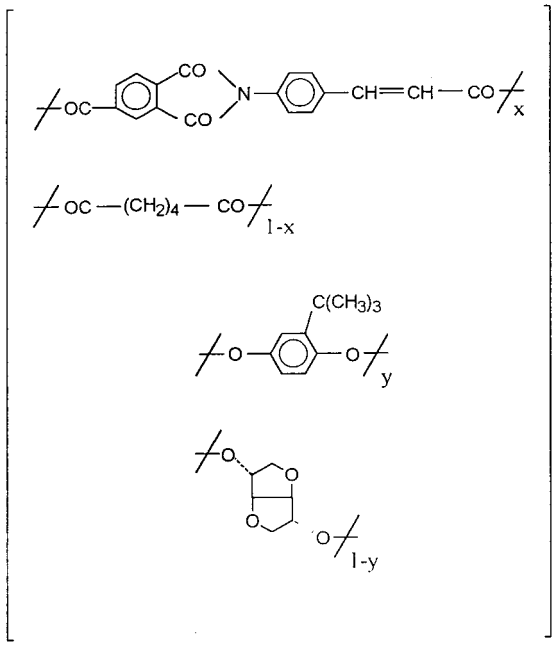

7

7a: x=0.6
y=0.95
7b: x=0.8
y=0.95
7c: x=1
y=0.95

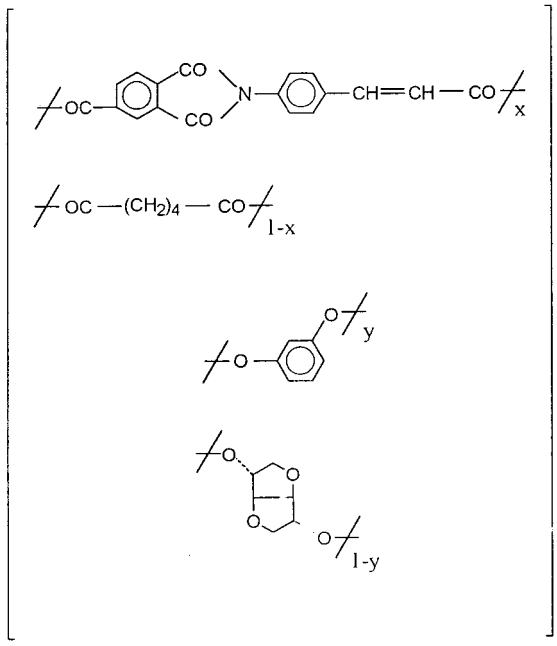

8

8a: x=0.6
y=0.95
8b: x=0.8
y=0.95
8c: x=1
y=0.95

for PEN in the temperature range between the β- and the α-relaxation a β'-process has been observed which was related to molecular motions of aggregates of the naphthalene groups.[14,15] Moreover, for poly(amide imide)s in addition to the β-relaxation, a β'- and an

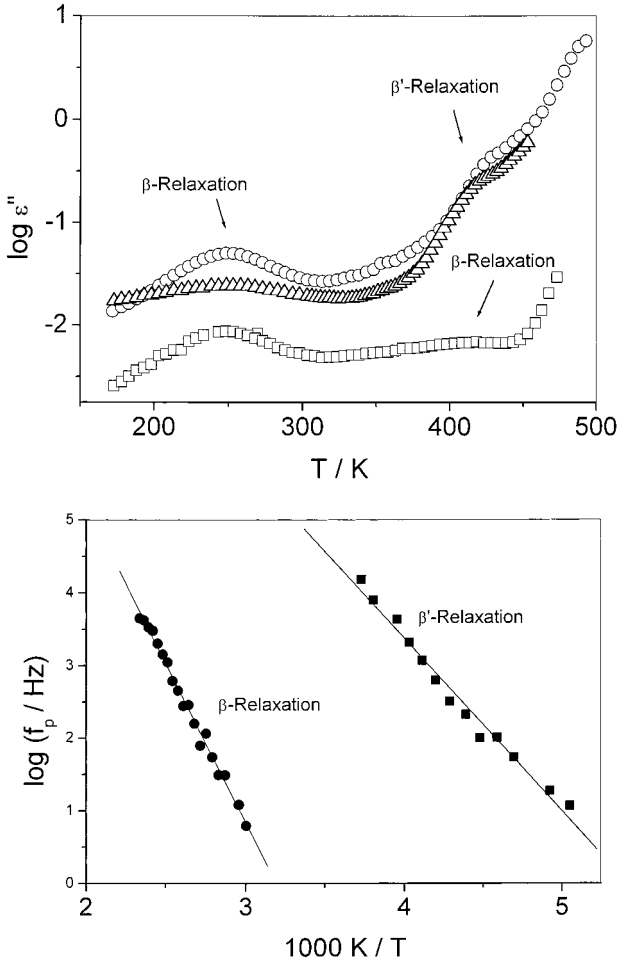

Figure 2. (a) Log ϵ'' vs temperature for the copolymers (□) **7c**, (○) **7b**, and (△) **7a.** (b) Log f_p vs $1/T$ for the polymer **7c**: □, β'-relaxation; ■, β-relaxation. Lines are fits of eq 2 to the data.

α′-relaxation process have been observed at temperatures below the dynamic glass transition.[16]

In Figure 2a the logarithm of the dielectric loss ϵ'' vs the temperature at a fixed frequency of 1000 Hz is shown for the polymers **7a**−**7c**. Two relaxation processes can be observed. A β-relaxation process is indicated by a peak of ϵ'' for all investigated polymers at approximately 250 K. Its relaxation strength depends strongly on structure. At higher temperatures but below T_g a further relaxation process is indicated by a shoulder in ϵ'' for the samples **7a** and **7b**. Because this process is observed at temperatures below the glass transition temperature it is called β'-relaxation. For the polymers **7a** and **7b** that process is followed by a further increase of the dielectric losses which can be due to the low-temperature tail of the α-relaxation. In the case of the polymer **7c** a very weak peak is detected in the same temperature range followed also by a further increase of ϵ''.

The relaxation strength of the β-relaxation depends clearly on the structure. It is observed also for sample **7c**, which does not contain the flexible $-(CH_2)_4-$ group. This means first of all that the β-relaxation cannot be assigned to molecular fluctuations of this group. Moreover, the CH_2 units have a very weak dipole moment, and so molecular fluctuations of it can be hardly detected by dielectric spectroscopy. Second, the intensity of the β-process increases with the concentration of the flexible spacer group. It can be argued that the molecular mobility of the groups which are responsible for the β-relaxation or its number is enhanced by the $-(CH_2)_4-$ units. For the highest concentration of alkyl groups the β-absorption becomes very broad. Assuming that the width of a relaxation peak can be attributed to a distribution of relaxation times or rates which are caused by a distribution of different environments, one can conclude that the highest concentration of the $-(CH_2)_4-$ units causes a more heterogeneous molecular structure than in cases of lower concentrations. Probably, the higher flexibility of the chain and the incompatibility of the different constituents causes a kind of nanophase separation. Also, the change in the dielectric strength of the β-relaxation is in agreement with that interpretation. A similar phenomenon was observed for poly(*n*-alkyl metharylate)s with longer side chains.[32]

Table 4. Activation Energy E_A and log f_∞ for the β- and β'-Relaxation of Polymers 7a−7c

	β-regime		β'-regime	
polymer	E_A/kJ mol^{-1}	log(f_∞/Hz)	E_A/kJ mol^{-1}	log(f_∞/Hz)
7c	46	13	84	14
7b	45	13		
7a	55	13	67	10

The model function of Havriliak−Negami (HN function)[33] is fitted to the isothermal data[34] to parametrize the β-process. So the relaxation rate at maximal loss $f_{p\beta}$ can be determined. As an example $f_{p\beta}$ vs inverse temperature (Arrhenius diagram) is plotted for the sample **7c** in Figure 2b. The temperature dependence of log $f_{p\beta}$ can be described by an Arrhenius equation which reads

$$\log(f_p) = \log(f_\infty) - \frac{2.3E_A}{k_B T} \qquad (1)$$

where E_A is the activation energy, f_∞ is the preexponential factor, and k_B is the Boltzmann constant.

The calculated activation parameters of the β-relaxation are given in Table 4. The value of the estimated activation energy is relatively low and indicates that the underlying motional process is local in nature. For the polymer **7a** a slightly higher value is obtained. A quite similar value was found for the β-relaxation process for PET and PEN. So it can be assumed that the CO unit which has a considerable dipole moment is responsible for the β-relaxation on a molecular level.

Also, the intensity of the β'-process depends on the structure of the polymer under investigation. In the case of high concentration of the flexible spacer group the dielectric strength of the β'-process is essentially higher than for the sample **7c** which does not contain CH_2 units. But because the β'-process is also observed for this sample, the molecular origin of it has to be attributed to the chain unit which is present in that polymer.

Also, the β'-relaxation process can be analyzed by fitting the HN function to the data (Figure 2b). As for the β-process also for the β'-relaxation the data can be described by the Arrhenius equation. But in contradiction to the β-absorption the estimated activation energies (see Table 4) are rather high for a local motional process. Therefore, it is concluded that the β'-relaxation should be related to a bulky molecular unit. The cinnamoyl unit can be excluded because of the weak dipole moment. More likely is that the bulky imide unit is responsible for the β'-relaxation. This interpretation is first favored by the high dipole moment of that group

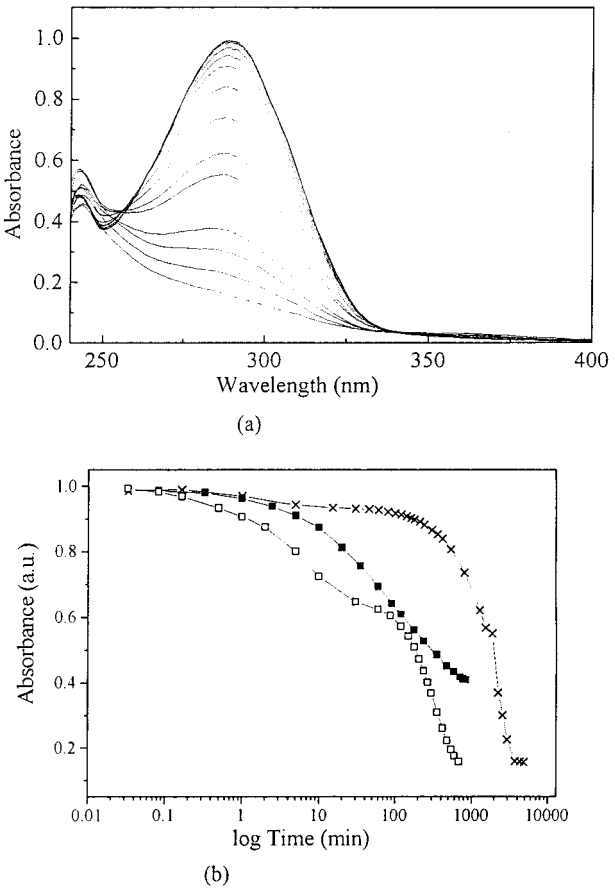

Figure 3. (a) Change of absorption spectra caused by the photolysis of **3** in $CHCl_3$ upon UV irradiation (313 nm, 2,5 mW/cm^2, t = 0−5000 min). (b) Normalized absorption−time diagram in a log scale of **3** in solution (×) at 289 nm, **7c** in solution (□), and as spin-coated film (■) at 298 nm.

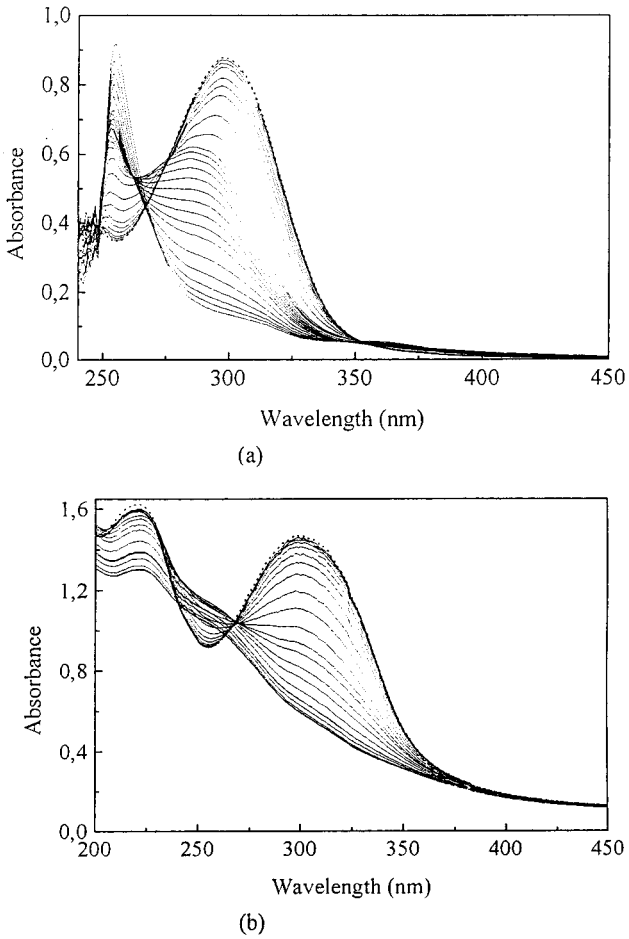

Figure 4. Change of absorbance of **7c** upon UV irradiation (a) in $CHCl_3$/TFA and (b) as spin-coated film, whereas the dotyed line shows the initial spectra.

and, second, by the line of argumentation that perhaps more groups contribute to the process and that these units become more mobile with increasing concentration of the $-(CH_2)_4-$ units. In addition, that conclusion is supported by the fact that the activation energy seems to decrease with increasing concentration of the spacer group (see Table 4). Another interpretation of the β'-relaxation is that the aromatic groups can form aggregates. Clearly the formation of aggregates is much easier for higher spacer concentration than for lower ones, and therefore the intensity of the β'-relaxation increases also in that picture with the number of CH_2 groups. A similar interpretation is used for the explanation of the β*-process in PEN. But one has to state that the activation energies are much lower in the here presented[15] case. To decide between both lines of argumentation to assign the β'-relaxation requires additional experiments.

Photochemical Behavior. The photochemical properties of the polyesters **7a**−**c** and the related monomeric model compound **3**, which contain all the same photochromic moiety, have been studied in solution and as spin-coated films. Figure 3 illustrates the change of the UV/vis absorbance of the ester **3** upon irradiation with UV light (313 nm) in $CHCl_3$. The initial spectrum is characterized by the absorption maximum of the $\pi\pi$* transition of the cinnamic ester moiety at 289 nm. In contrast to **3**, the monomer **1** with the *p*-phenylene diarylic moiety has its absorption maximum at 325 nm. The UV irradiation of **3** results in a decrease of this absorption band. The effect is caused by the *E*/*Z* photoisomerization establishing a steady state between the *E* and the *Z* isomeric form while the (2 + 2) photocycloaddition takes place simultaneously, forming cyclobutane rings of the truxinic or truxillic ester. An isosbestic point at 265 nm is observed at the beginning of the irradiation procedure which corresponds to the *E*/*Z* photoisomerization.

The time dependence of the photoconversion using a logarithmic scale (Figure 3b) demonstrates that there are two processes. So, photoisomerization and photocycloaddition can be distinguished clearly by the different kinetics of both processes in solution. Initially the steady state of *E*/*Z* photoisomerization is established rapidly at an A/A_0 value of about 0.93, which is in agreement with other studies of cinnamoyl moieties in polymeric films. The subsequent slower decrease of absorption indicates that the photocycloaddition reaction goes to a high conversion ($A/A_0 \approx 0.18$).

Figure 4a displays the change of the absorbance of the polymer **7c** in solution ($CHCl_3$/TFA) induced by the same irradiation procedure. Compared to monomer **3,** the initial absorption maximum of the polymer at 298 nm is 9 nm bathochromically shifted in the same solvent. The absorbance maximum of polymer **5** synthesized from the monomeric ester **1** is shifted about 14 nm to shorter wavelengths compared to the case of **1**. Upon UV irradiation, the absorbance at 298 nm decreases and that at 255 nm increases simultaneously. This is caused by the photocycloaddition resulting in a

cross-linking forming cyclobutane rings substituted with phenyl groups. In addition, a slow increase of the absorbance is observed between 352 and 450 nm. This change should be related to the photo-Fries reaction of the aromatic cinnamic acid ester unit forming 2-hydroxybenzophenone groups. At the beginning of the irradiation an isosbestic point at 270 nm is observed which should correspond to the *E*/*Z* photoisomerization and which is lost on continued irradiation.

Upon UV irradiation a similar decrease of the absorbance is found in the case of the spin-coated film of **7c** (Figure 4b). Initially, an isosbestic point is observed at 270 nm. The absorption at 255 nm increases in the first period but decreases after 4 h of irradiation. The spectral changes reach saturation values after 14 h, indicating a high conversion of the cycloaddition reaction which results in the photo-cross-linking of the films.

Figure 3b compares the decrease of the normalized absorption of **3** in solution with that of the polymer **7c** in solution and as spin-coated film. Using a logarithm scale, it is clearly seen that initially the photoisomerization dominates, but the photocycloaddition becomes more efficient in the case of the solved polymer compared to the monomer. This should be caused by the higher local concentration in the cinnamoyl group attached to the polymeric backbone. However, the efficiency of the main conversion is comparable to that of the monomeric ester. The instability between initial and final conversion which is found for all polymers in solution should be caused by light-induced changes of the configuration of the soluted macromolecule during the irradiation. So, the molecular photoreactions cause changes of polarity, shape, and intermolecular interaction which result in modified aggregation and dynamics. The last one is mainly caused by the cross-linking of the solved macromolecule. In the case of the spin-coated film such easy separation in the two processes is not possible. *E*/*Z* photoisomerization and photocycloaddition occur simultaneously caused, on one hand, by an increasing efficiency of the photocycladdition reaction by the high local concentration forming reactive sites and, on the other, by the restriction of the photoisomerization by matrix effects.

In Figure 5 the photochemical behavior of the polymers **7a**−**c** which differ in the ratio of the cinnamoyl group in the polymer composition is compared in solution (TFA/$CHCl_3$) and spin-coated films. In solution the two processes can be clearly indicated. The fast process, the *E*/*Z* photoisomerization, causes a prompt decrease of the absorption followed by a slower one. This decrease of absorbance should be caused by the photocycloaddition reaction as discussed. This behavior is observed in the case of all three polymers. An identical course of the normalized decrease of absorbance vs the time was found for all three polymers in the first period of exposure, while in the second part corresponding to the bimolecular photocycloaddition it is different for the three polymers in solution and in the films. In solution the conversion increases with increasing content of the cinnamoyl group in the copolymers, and the homopolymer has the maximum value (Table 5).

In contrast to the behavior in solution where two processes can be clearly distinguished, this is more complicated in the case of the films because the efficiency of the decrease of absorbance becomes more similar for both processes. General, the saturation value of the conversion is smaller in the glassy polymer films

Table 5. Maximum Conversion in % on UV Irradiation Measured at the Absorbance at 298 nm

	max conversion (%)	
ratio of cinnamoyl moiety (%)	solution	film
0.6	72.7	68.8
0.8	77.6	64.6
1.0	84.3	59.2

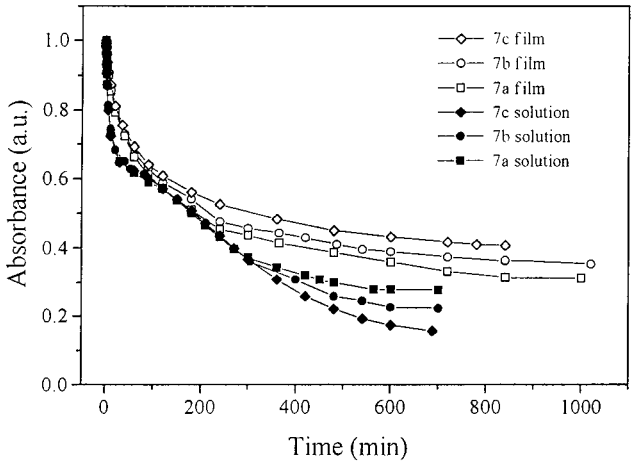

Figure 5. Absorption−time diagram of the photodegradation of **7a**−**c** in solution (open) and spin-coated films (close) at 298 nm upon UV irradiation.

compared to all three polymers in solution. In the solid matrix the conversion of about 68.8% is highest for the polymer with 0.6 of cinnamoyl units, that is, the lowest ratio of photochromic moieties under investigation. It is smallest in the case of the homopolymer. It shows that in glassy films the higher mobility of the copolymers caused by aliphatic ester groups is more important for a high conversion as a high concentration of the stiff rodlike cinnamoyl group. In this sense the photochemical behavior corresponds to the results found for the molecular dynamics measured by dielectric spectroscopy. The curves also indicate that nonreactive sites of cinnamoyl groups remain intact within the polymeric coil in solution and in the cross-linked polymer matrix of the glassy film. The part of nonreactive sites is greater in solid films compared to the solution.

Optical anisotropy is induced, irradiating a spin-coated film of polymer **7a** with linearly polarized light of a HeCd laser (325 nm, 10 mW/cm^2). As shown in Figure 6, a dichroism of about 0.07 is generated, observing the absorption band of the cinnamoyl group at 298 nm.

Initially, the value increases proportional to the absorbed energy and reaches a saturation value after 90 min. The maximum value is observed at a conversion of 0.36. The question which of the photoreactions contribute mainly to the anisotropy cannot be answered in the moment. The photoinduced anisotropy in the film corresponds to dichroic ratios which were found upon irradiation of cinnamoyl-containing side chain polymers such as poly(vinyl cinnamate). The photoinduced dichroism in the film of **7a** remains constant on subsequent irradiation, establishing a saturation value of conversion at 0.56. On storage the film for 5 days at room temperature the dichroism is decreased only slightly to a value of 0.05. In contact with the liquid crystal 5CB the photoanisotropic interface of the films causes the alignment of liquid crystals.

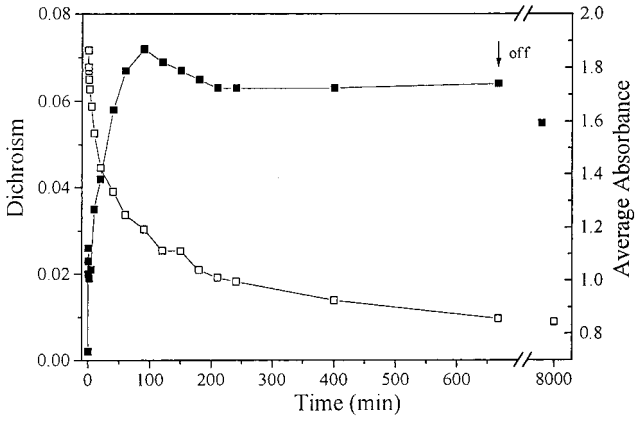

Figure 6. Dichroism (■) and average absorbance (□) of **7a** after irradiation with linearly polarized light (325 nm, 10 mW/cm^2).

In this way, the liquid crystal becomes planar aligned, whereas the anisotropy in this films is significantly higher compared to that which is caused by rubbing or, alternatively, by irradiation of polyimide films with linearly polarized UV light.

Conclusion

Liquid crystalline poly(ester imide)s with cinnamoyl moieties and chiral groups as part of the backbone were synthesized and characterized concerning their liquid crystalline, dynamic, and photochemical properties. The copolymers are cholesteric, but exclusively the polymers containing the *tert*-butylhydroquinone moiety form blue iridescent Grandjean textures on annealing. The solubility of the polymers is poor, and in this way their capability to form homogeneous films is a problem.

UV irradiation causes a photo-cross-linking of the polymers via the (2 + 2) photocycloaddition of the cinnamoyl moieties, resulting in insoluble films. The process results in a freezing-in of the supramolecular structure of the Grandjean texture with its iridescent color without any changes compared to the initial films. In the glassy films the molecular dynamics and the photoconversion increases from the stiff homopolymer to the more flexible copolymers with increasing concentration of the adipinic ester as spacer in the backbone. Upon irradiation with linearly polarized UV light a dichroism of about 0.07 is induced in films of these photochromic poly(ester imide)s, which is much higher as observed for the irradiated polyimide films and which is comparable with that of other cinnamoyl-containing polymers.[32] The photoinduced anisotropy in the films interface causes an efficient alignment of liquid crystals.

References and Notes

(1) Boulignand, Y. *J. Phys. (Paris)* **1993**, *34*, 603.
(2) de Jeu, A. W.; Verteugen, G. *Thermotropic Liquid Crystals, Fundamentals*; Springer-Verlag: Berlin, 1977.
(3) Ichimura, K. *Chem Rev.* **2000**, *100*, 1847.
(4) Schadt, M.; Schmitt, K.; Kozinkov, V.; Chigrinov, V. *Jpn. J. Appl. Phys.* **1992**, *7*, 2155.
(5) Marusii, T. Y.; Reznikov, Y. A. *Mol. Mater.* **1993**, *3*, 161.
(6) Ichimura, K.; Akita, Y.; Akiyama, I.; Hayashi, Y.; Kudo, K. *Jpn. J. Appl. Phys.* **1996**, *35*, L992.
(7) Kawatsuki, N.; Ono, H.; Takatsuka, H.; Yamamoto, T.; Sangan, O. *Macromolecules* **1997**, *30*, 6680.
(8) Hasagawa, M.; Taira, Y. *J. Photopolym. Sci. Technol.* **1995**, *8*, 703.
(9) West, D. L.; Wang, X. D.; Ji, Y.; Kelly, J. R. *Proc. SID* **1995**, *26*, 703.
(10) Wang, X. D.; Subacius, D.; Lavrentovich, O.; West, J. L.; Reznikov, Y. *Proc. SID* **1996**, *27*, 654.
(11) Carius, H.-E.; Schönhals, A.; Guigner, D.; Sterzynski, T.; Brostow, W. *Macromolecules* **1996**, *29*, 5017.
(12) Spies, C.; Gehrke, R. *Macromolecules* **1997**, *30*, 1701.
(13) Johnes, A. S.; Dickson, T. J.; Wilson, B. E.; Duhamel, J. *Macromolecules* **1999**, *32*, 2956.
(14) Canadas, J. C.; Diego, J. A.; Sellares, J.; Mudarra, M.; Belania, J.; Diaz-Calleja, R.; Sanchis, M. J. *Polymer* **1999**, *40*, 1181.
(15) Hardy, L.; Stevenson, I.; Boiteux, G.; Seytre, G.; Schönhals, A. *Polymer* **2001**, *42*, 5679.
(16) Stauga, R.; Schönhals, A.; Carius, H.-E.; Mudrak, C. V.; Privalko, V. P. *New Polym. Mater.* **1998**, *5*, 119.
(17) Schönhals, A. In *Dielectric Properties of Amorphous Polymers in Dielectric Spectroscopy of Polymeric Materials*; Runt, J., Fitzgerald, J., Eds.; American Chemical Society: Washington, DC, 1997.
(18) Stumpe, J.; Zaplo, O.; Kreysig, D.; Niemann, M.; Ritter, R. *Makromol. Chem.* **1992**, *193*, 1567.
(19) Fischer, Th.; Läsker, L.; Rutloh, M.; Czapla, S.; Stumpe, J. *Mol. Cryst. Liq. Cryst.* **1997**, *299*, 293.
(20) Stumpe, J.; Fischer, Th.; Menzel, H. *Macromolecules* **1996**, *29*, 2831.
(21) Rutloh, M.; Stumpe, J.; Stachanov, L.; Kostromin, S.; Shibaev, V. *Mol. Cryst. Liq. Cryst.* **2000**, *352*, 149.
(22) Preston, J.; Dewinter, W.; Black, W. B. *J. Polym. Sci., Polym. Chem. Ed.* **1972**, *10*, 1377.
(23) Ruggli, P.; Teilheimer, W. *Helv. Chim. Acta* **1941**, *24*, 899, 916.
(24) Kricheldorf, H. R.; Probst, N. *Macromol. Chem. Phys.* **1995**, *196*, 3511.
(25) Kricheldorf, H. R.; Probst, N.; Wutz, Chr. *Macromolecules* **1995**, *28*, 7990.
(26) Schönhals, A.; Kremer, F.; Schlosser, E. *Phys. Rev. Lett.* **1991**, *67*, 999.
(27) Kricheldorf, H. R.; Probst, N. *High Perform. Polym.* **1995**, *7*, 471.
(28) Schwarz, G.; Kricheldorf, H. R. *J. Polym. Sci., Part A: Polym. Chem.* **1996**, *34*, 603.
(29) Kricheldorf, H. R.; Kratwinkel, T. *High Perform. Polym.* **1997**, *9*, 121.
(30) Stumpe, J.; Ziegler, A.; Berghahn, M.; Kricheldorf, H. R. *Makromolecules* **1995**, *28*, 5306.
(31) Kricheldorf, H. R.; Gerken, A.; Yulbichaev, B.; Friedrich, C. *J. Polym. Sci., Part A: Polym. Chem.* **2000**, *38*, 2013.
(32) Sapich, B.; Stumpe, J.; Gerus, I.; Yaroshchuk, O. *Mol. Cryst. Liq. Cryst.* **2000**, *352*, 9.
(33) Havriliak, S.; Negami, S. *J. Polym. Sci., Polym. Symp.* **1966**, *14*, 89.
(34) Schlosser, E.; Schönhals, A. *Colloid Polym. Sci.* **1989**, *267*, 963.
(35) Beiner, M., personal comunications.

MA001616B